Solute Dependence of Three Pulse Photon Echo Peak Shift Measurements in Methanol Solution

Yutaka Nagasawa,* Ayako Watanabe, Hiroko Takikawa, and Tadashi Okada

Department of Chemistry, Graduate School of Engineering Science and Research Center for Materials Science at Extreme Conditions, Osaka University, Toyonaka, Osaka 560-8531, Japan

Received: October 8, 2002; In Final Form: November 29, 2002

Three pulse photon echo peak shift (3PEPS) measurement has recently become a popular method to study solvation and protein dynamics. In this paper, dependence of the 3PEPS signal on probe solute molecules was studied using several xanthene dyes and styryl dye molecules in methanol and compared with pump−probe measurements. For xanthene dyes, the decay was faster when the blue side of the absorption spectrum was excited. This effect is considered to be the result of a limited observation window and vibrational relaxation of the excess energy through higher density of states in the excited state. Nonlinear coupling may be also need to be considered. It seemed that the 3PEPS signal was more sensitive to excited state dynamics rather than to the ground state ones. For styryl dyes, a gradual increase of the peak shift was observed in the picosecond region, which may be the result of photoinduced isomerization.

1. Introduction

Solvation dynamics has been studied extensively because of its importance in condensed phase chemical reactions.[1−9] It is usually studied using a nonreactive solute−solvent system, of which the solute molecule changes its value of electric dipole moment on photoexcitation. When the solute molecule is excited by a short laser pulse, the dipole moment instantaneously changes its value and/or direction. Intramolecular nuclear configuration and solvent orientation will change subsequently after the photoexcitation, because nuclear and molecular motions are slower than those of electrons. Solvation dynamics usually takes place in the picosecond time scale, and it can be measured by spectroscopic methods such as time-resolved fluorescence dynamic Stokes shift (FDSS),[3,4,7] hole burning,[10−12] or three pulse photon echo peak shift (3PEPS) measurements.[13−18] Solvation dynamics on the excited state causes the energy gap between the ground and the excited state to reduce with time, and the energy relaxation process exhibits itself as a time-dependent red shift of the emission. On the other hand, when the exciting laser bandwidth is narrower than the inhomogeneous bandwidth of the ground state absorption spectrum, a hole can be burnt in the spectrum and the ground state solvation dynamics can show up as a time-dependent broadening of the hole. The 3PEPS measurement monitors the peak shift between two echo signals appearing in the phase-matched direction of $-\mathbf{k}_1 + \mathbf{k}_2 + \mathbf{k}_3$ and $\mathbf{k}_1 - \mathbf{k}_2 + \mathbf{k}_3$ as a function of the population period, i.e., the delay between the second and the third optical pulses. The peak shift decreases as the solvation process proceeds.

When the FDSS is measured, solvation dynamics is represented by a spectral shift correlation function[1−9]

$$S(t) = \frac{\nu(t) - \nu(\infty)}{\nu(0) - \nu(\infty)} \tag{1}$$

where $\nu(t)$ is the peak frequency of the fluorescence spectrum at time t. For hole-burning measurement, it is represented by a bandwidth correlation function[11,19]

$$W(t) = \sqrt{\frac{\sigma(t)^2 - \sigma(\infty)^2}{\sigma(0)^2 - \sigma(\infty)^2}} \tag{2}$$

where $\sigma(t)$ is the bandwidth of the spectrum at time t. When linear response and high temperature limit are assumed, these functions are approximately equivalent to the solvent fluctuation correlation function of the electronic transition energy

$$M(t) = \frac{\langle \delta\omega_{eg}(0)\, \delta\omega_{eg}(t) \rangle}{\langle \delta\omega_{eg}{}^2 \rangle} \tag{3}$$

where $\delta\omega_{eg}(t)$ is the fluctuation of the transition frequency. For the 3PEPS measurement, the relation between the $M(t)$ and the photon echo peak shift, $\tau^*(t)$, is approximated to be[20,21]

$$\tau^*(t) = \frac{M(t)}{\sqrt{\pi[\langle \Delta^2 \rangle + \lambda^2 f(t)]}} \tag{4}$$

where $\langle \Delta^2 \rangle$ is the coupling strength and λ is the reorganization energy with $f(t) = [1 - M(t)]^2$. When $M(t)$ exhibits bimodal dynamics with a dominant fast initial part and a slower tail, $M(t) = (1 - a)M_{fast}(t) + aM_{slow}(t)$ with $a \ll 1$, and the relation between the peak shift and the slow part of the correlation function becomes[17,21]

$$\tau^*(t) \approx \frac{aM_{slow}(t)}{\sqrt{\pi(\langle \Delta^2 \rangle + \lambda^2)}} \tag{5}$$

Many efforts have been made to extract $M(t)$ and to obtain time scales of solvation dynamics from these experimental

10.1021/jp0271559 CCC: $25.00
Published on Web 01/07/2003

methods. The solvation process can be roughly separated into two components, i.e., the inertial component, which appears in the time scale shorter than 100 fs, and the diffusive component, which appears in the picosecond time region.[1,3,5,6,8] The inertial component is caused by the small angle free rotation of a few solvent molecules within the first solvation shell, while the diffusive component is caused by the diffusive rotation and translation of the bulk solvent. The inertial component is often approximated by a Gaussian function because the time differential at time origin has to be zero.[22] The diffusive component is usually expressed by a multiexponential or stretched exponential function, which may be ascribed to the time-dependent dielectric friction or to the hierarchy structure of the solvation shell.

However, the common problem among these methods is that because they always utilize some probe solute molecule, $M(t)$ not only contains solvation dynamics but also contains intramolecular contributions. The ultrafast inertial contribution to the solvation dynamics was first observed by a dye, styryl 7 (LDS750), dissolved in acetonitrile.[22] However, styryl 7 is rather a floppy molecule with multidimensional rotational freedom, which may lead to photoinduced isomerization. It was pointed out that the stationary emission band has a width (full width at half-maximum, fwhm) of 1490 cm^{-1} while the absorption band is 4600 cm^{-1} wide. This deviation from mirror symmetry has led to concern about the use of styryl dyes as solvatochromic probes.[3,23] Transient absorption and gain measurement was carried out for styryl 7, and it was concluded that an intramolecular process dominates the observed Stokes shift.[24] The first excited electronic state isomerizes in an ultrafast process followed by a slower process, the dynamics of which is controlled by the solvent. Coumarin dyes, which are rigid molecules with much less freedom to rotate, have been used extensively as probe molecules by Barbara, Fleming, Maroncelli, and others.[1−9] However, even for coumarin dyes, there are some criticisms that they are not a perfect probe for solvation dynamics. Transient absorption and gain spectra of coumarin 153 were compared to the results from semiempirical calculations for higher excited states, and it was concluded that they are not fully consistent with relaxation due to pure solvation and may indicate an intramolacular process.[25,26] It should also be pointed out that coumarins 153 and 337 were found to exist in two conformations under supersonic jet conditions.[27] Semiempirical calculations suggested structure assignments corresponding to syn and anti conformations of the saturated ring on the amino group.

Chapman et al. have carried out time-resolved Stokes shift measurements to measure the solvaiton times of 16 different probe solutes, including coumarins, in a single solvent, 1-propanol (253 K).[28] Rather than exhibiting a continuous range of solvation times, the dynamics indicated a division of these probe molecules into two distinct classes. The majority (11) of the solutes was observed to fall into a "normal" category. The solvation times of these solutes span a relatively narrow range, 0.14−0.22 ns, times consistent with expectations based on nonspecific theories of solvation dynamics. The remaining five solutes, all simple aromatic amines, formed a distinct group whose solvation dynamics was at least 2-fold faster than those of the normal solutes. The difference between these two classes of solutes appeared to reflect differences in the nature of their hydrogen-bonding interactions with the solvent. This result indicated that even in the presence of intramolecular relaxation, careful selection of solute molecule enables one to measure substantial solvation time.

Recently, 3PEPS measurement has become a popular method to study dynamics of solvation, protein matrix, and others.[13,15−17,20,21,29−50] However, solute dependence of this method has never been examined carefully. Large flexible molecules with large degrees of rotational freedom, such as IR144 and DTTCI, are often used in this method.[16,17] In the present study, we have carried out 3PEPS measurements of six xanthene dyes and two styryl (hemicyanine) dyes in methanol solution at room temperature. The 3PEPS signal exhibited a rather complicated solute dependence. The signals of xanthene dyes showed a correlation with the absorption peak wavelength, i.e., the peak shifts were smaller and 3PEPS decays were faster for dyes with longer absorption wavelengths. This effect is considered to be the result of a limited observation window and vibrational relaxation (VR) of the excess energy through higher density of states.[51] For styryl dyes, a gradual increase of the peak shift was observed in the picosecond region, which may be the result of photoinduced isomerization.

2. Experiment

The details of the homemade cavity-dumped Kerr lens modelocked Cr:forsterite laser were reported elsewhere.[52] The cavity-dumping efficiency was about 30%, and the repetition rate was fixed to 100 kHz. The cavity-dumped beam was focused into a 4 mm LBO crystal to convert the fundamental frequency of 1270 nm into the second harmonic at 635 nm. The conversion efficiency was 20−30%, and the second harmonic pulse energy was ∼5 nJ. The autocorrelation trace of the second harmonic pulse was measured by a 0.1 mm BBO crystal with the same setup used for the 3PEPS experiment. The measured fwhm of each of the three pulses was ∼33 fs. The 3PEPS experimental setup was almost identical to the one reported previously.[16,34,53] The optical path of the sample cell was 0.5 mm, and the optical density of the sample was ∼1.2 at the absorption peak. A homemade rotating cell was used to avoid optical damage of the sample. The averaged energy of three pulses was ∼0.6 nJ, which was low enough to avoid unwanted higher order nonlinear effects.[16,29] When the energy was reduced to ∼0.3 nJ, the signal became significantly noisy, although the echo peak shift or the overall feature of the degenerate four wave mixing signal did not change. Concentration dependence was also checked from 2.6×10^{-4} to 6.6×10^{-5} M, and the echo peak shift or the overall feature of the degenerate four wave mixing signal did not change. The pulses were focused into the sample by a 10 cm focusing achromatic lens. The signals were detected by photodiodes (New Focus, model 2031) and lock-in amplifiers (EG&G Instruments, model 5210).

In 3PEPS measurement, both echo signals at phase-matching conditions, $\mathbf{k}_1 - \mathbf{k}_2 + \mathbf{k}_3$ and $-\mathbf{k}_1 + \mathbf{k}_2 + \mathbf{k}_3$ are simultaneously recorded. Because there are three pulses, there are three time periods to consider, of which only the first two are under experimental control. The first time period, τ, during which the system is in an electronic superposition state, is scanned. During the second time period, T, the system is in a diagonal population state. This is the key feature of the experiment, which gives its large dynamic range. The third pulse creates the final superposition, which leads to rephasing and echo formation. This last period is integrated to record the echo intensity as a function of τ. The observation of interest is the location of the echo maximum with respect to zero delay, $\tau = 0$ fs, for different fixed values of T. The shift from zero delay, $\tau^*(T)$, is what we refer to as the peak shift, and by measuring both phase-matched echoes simultaneously, this can be recorded with extremely high precision. When the signal intensity was strong, the accuracy of $\tau^*(T)$ was as high as ±0.3 fs; however, when the population

SCHEME 1: Molecular Structures of the Dyes

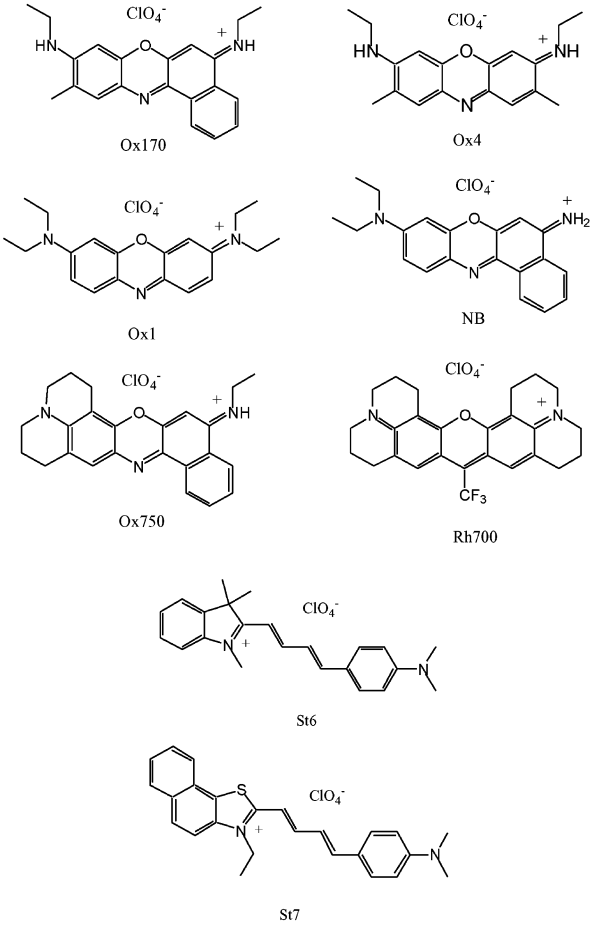

period was elongated and the signal intensity became weak, the accuracy was as low as ±1.0 fs for some cases. The peaks of the echo signals are estimated by fitting with a Gaussian function. A plot of $\tau^*(T)$ vs T constitutes a 3PEPS data set.

The details of the pump−probe (PP) experimental setup were described elsewhere. [54] The measured fwhm of the pulse was ~33 fs. The energy of the pump pulse was ~1.0 nJ and that of the probe pulse was ~0.1 nJ. The pulses were focused into the sample by a 5 cm focusing lens. A homemade rotating cell was used to avoid optical damage of the sample. The optical path of the sample cell was 0.5 mm, and the optical density of the sample was ~1.2 at the absorption peak. The signals were detected with and without a monochromator by a photodiode (New Focus, model 2031) and a lock-in amplifier (EG&G Instruments, model 5210). The optical delay between the pump and the probe pulses was scanned up to 120 ps, which was the same range as the 3PEPS scan.

Oxazine 1 (oxazine 725), oxazine 4 (LD690), oxazine 170 (oxazine 720), oxazine 750, Nile blue, rhodamine 700 (LD700), styryl 6 (LDS730), and styryl 7 (LDS750) were purchased from Exciton Chemicals and used without further purification. Methanol was infinity pure grade from Wako Pure Chemical Industries. Absorption and fluorescence spectra were measured by Hitachi U-3500 spectrophotometer and 850E spectrofluorometer, respectively.

3. Results

Scheme 1 and Figure 1 show the molecular structure and absorption and fluorescence spectra of xanthene dyes, oxazine 1 (Ox1), oxazine 4 (Ox4), oxazine 170 (Ox170), oxazine 750 (Ox750), Nile blue (NB), and rhodamine 700 (Rh700). The

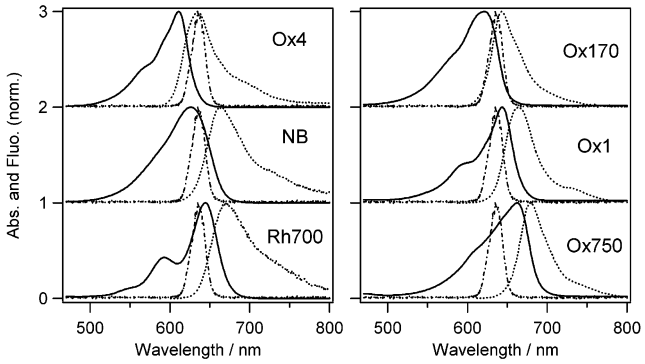

Figure 1. Normalized absorption (solid curve) and fluorescence spectra (dotted curve) of xanthene dyes in methanol solution. Spectrum of the excitation pulse (dash-and-dotted curve) is also shown for comparison.

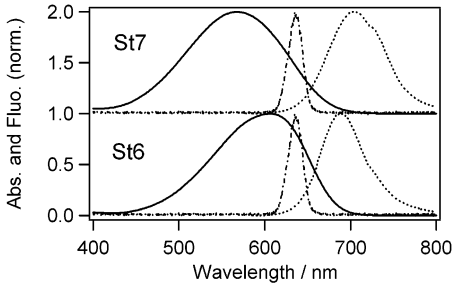

Figure 2. Normalized absorption (solid curve) and fluorescence spectra (dotted curve) of styryl dyes in methanol solution. Spectrum of the excitation pulse (dash-and-dotted curve) is also shown for comparison.

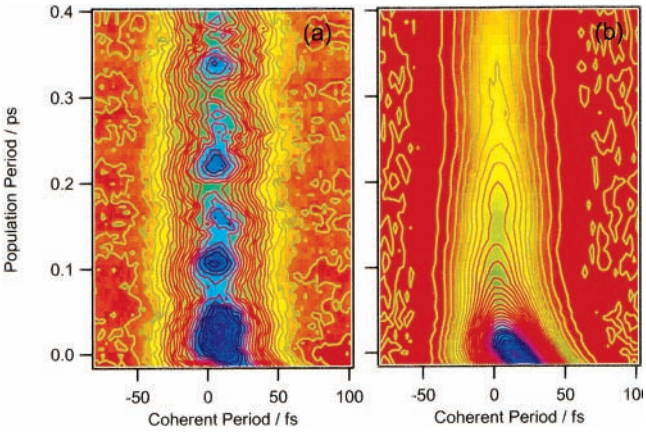

Figure 3. Two-dimensional plot of the degenerate four wave mixing signal of (a) Ox4 and (b) St6 in methanol. Signal intensity is the highest at blue parts and lowest at red parts.

spectrum of the excitation laser pulse centered at 635 nm is also shown for comparison. The excitation pulse has the largest overlap with the fluorescence spectrum of Ox4 and Ox170 while the smallest is with that of Ox750 and Rh700. Absorption and fluorescence spectra of styryl dyes, styryl 6 (St6) and styryl 7 (St7), are shown in Figure 2. It can be seen that these dyes have a wider spectral width and larger Stokes shift between the absorption and the fluorescence peaks as compared to those of xanthene dyes.

When a degenerate four wave mixing signal is measured as a function of τ and T, the signal intensity can be plotted two-dimensionally as shown in Figure 3. Figure 3a,b represents a two-dimensional plot of the four wave mixing signals of Ox4 and St6, respectively, measured at the phase-matched direction of $-\mathbf{k}_1 + \mathbf{k}_2 + \mathbf{k}_3$. The horizontal cross-section of these signals is the three pulse photon echo signal, while the vertical cross-section along $\tau = 0$ fs is the transient grating signal. The shape

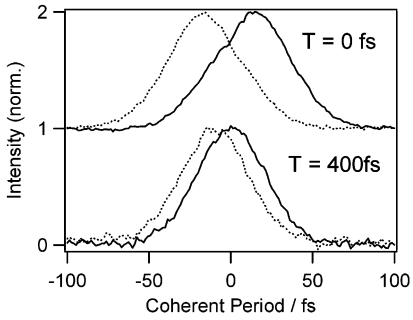

Figure 4. Stimulated echo signal of Nile blue in methanol detected in the phase-matching direction of $\mathbf{k}_1 - \mathbf{k}_2 + \mathbf{k}_3$ (dashed curve) and $-\mathbf{k}_1 + \mathbf{k}_2 + \mathbf{k}_3$ (solid curve) at $T = 0$ and 400 fs, respectively.

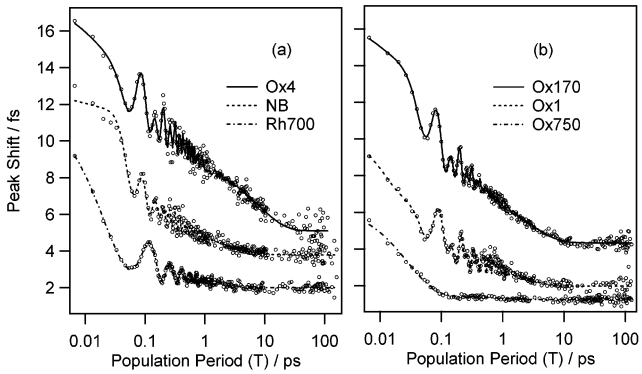

Figure 5. 3PEPS signals of xanthene dyes in methanol solution.

of the echo signal itself does not give much information, because optical dephasing is extremely fast and echo signal is practically symmetric in room temperature liquids. The quantity we are interested is the shift of the echo intensity peak from $\tau = 0$ fs. In Figure 4, echo signals of NB in methanol detected at both phase-matching directions of $\mathbf{k}_1 - \mathbf{k}_2 + \mathbf{k}_3$ and $-\mathbf{k}_1 + \mathbf{k}_2 + \mathbf{k}_3$ are plotted as a function of τ at $T = 0$ and 400 fs. It can be seen that the distance between the two peaks decreased when T was increased from 0 to 400 fs. The half of the separation between the two echo peaks plotted against T constructs the 3PEPS signal. The 3PEPS signals constructed for xanthene dyes in methanol are plotted in Figure 5 with the fitting result. The 3PEPS signals for styryl dyes are shown in Figure 6.

The fitting of the 3PEPS signals was carried out first with eq 5 and then with eq 4. Both fittings gave similar time constants. The $M(t)$ contains both vibrational and diffusive contributions

$$M(t) = \sum_i A_i \cos(\omega_i t + \phi) \exp(-t/\tau_i) + \sum_j A_j \exp(-t/\tau_j) \quad (6)$$

Frequencies of the vibrations, ω_i, were taken from the Fourier-transformed spectra of the PP signals of the dyes shown in Figures 8 and 9. For the inertial component of the solvation, the Gaussian function is often used for approximation. However, in our case, exponential function is also used for this component for simplicity. The fitting results are listed in Table 1. All of the signals needed more than two decay components. The fastest decay, which occurs within 100 fs, includes the inertial component of the solvation and destructive interference of the intramolecular wave packets. The time constant of this decay does not directly reflect the actual relaxation process because the pulse duration effect is present and eq 4 does not hold at short time scales, i.e., 100 fs. The slower decay components are free of such problems, and they are caused by diffusive solvation dynamics. In our analysis, we did not attempt to obtain

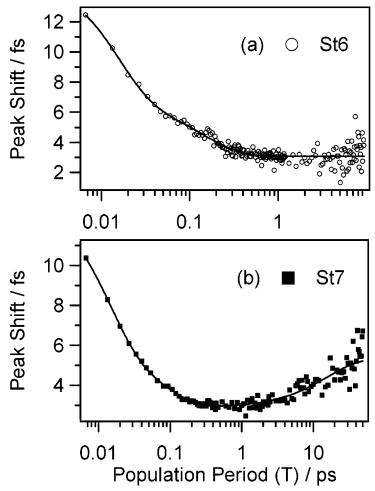

Figure 6. 3PEPS signals of (a) St6 and (b) St7 in methanol solution.

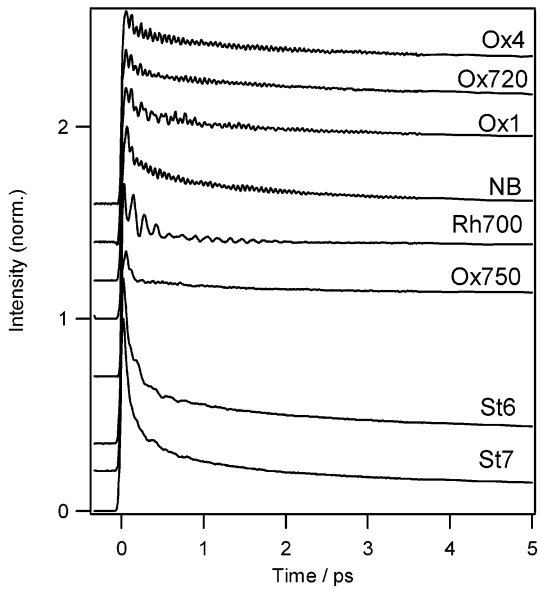

Figure 7. PP signals of the dyes in methanol.

the values of reorganization energy or coupling strength, because if the 3PEPS signal strongly depends on excitation wavelength,[29,30] the analysis will not result in quantitative determination of such parameters. We will only attempt to determine the time scales of the solvation process.

PP signals of the dyes are plotted in Figure 7. The difference transmittance of the probe pulse was measured as a function of delay between the pump and the probe pulses. Intramolecular coherent vibtrations can be clearly observed. The real parts of the Fourier-transformed spectra of these signals, which correspond to the resonance Raman spectra, are shown in Figures 8 and 9. The frequencies of the modes observed in these spectra were used for the fitting of the 3PEPS signals. A wavelength-resolved PP signal was also measured by setting a monochromator in front of the photodiode. The wavelength-resolved PP signals for Ox4 and Rh700 are plotted in Figure 10.

4. Discussion

4.1. Molecular Structures and Fourier-Transformed Spectra of the Dyes. Molecular structures of the dyes are shown in Scheme 1. Ox4, Ox1, and Rh700 have a C_2 symmetry. All of the xanthene dyes except Rh700 have free rotating amino groups. One of the amino groups of Ox750 is fixed with a saturated hexagonal alkyl ring, while both amino groups are

TABLE 1: Time Constants (τ_i) and Amplitudes (A_i) of the Decay Components Obtained from the Nonlinear Least-Squares Fitting of the 3PEPS Signals of the Dyes in Methanol Solution[a]

	Ox4	Ox170	NB	Ox1	Rh700	Ox750	St7	St6
λ_{abs} (nm)	611	620	626	644	644	662	567	606
λ_{flu} (nm)	634	643	664	664	671	697	705	689
Δ_{Stokes} (cm^{-1})	594	577	914	468	625	378	3450	1990
τ_1 (fs) (A_1)	41 ± 13 (0.33)	38 ± 5 (0.45)	35 ± 8 (0.74)	13 ± 6 (0.46)	12 ± 4 (0.47)	33 ± 10 (0.71)	14 ± 4 (0.46)	13 ± 6 (0.56)
τ_2 (fs) (A_2)	490 ± 90 (0.16)	400 ± 60 (0.14)		90 ± 20 (0.20)	110 ± 10 (0.23)		90 ± 30 (0.19)	150 ± 20 (0.22)
τ_3 (ps) (A_3)	8.4 ± 1.6 (0.20)	3.0 ± 0.3 (0.15)	1.1 ± 0.1 (0.26)	1.8 ± 0.2 (0.14)	1.5 ± 0.2 (0.07)	1.1 ± 0.6 (0.04)	16 ± 13 (−0.16)	
τ_4 (ps) (A_4)	≫100 (0.31)	≫100 (0.26)	≫100 (0.23)	≫100 (0.20)	≫100 (0.23)	≫100 (0.25)	≫50 (0.35)	≫10 (0.22)

[a] Absorption (λ_{abs}), fluorescence (λ_{flu}) maxima, and Stokes shifts (Δ_{Stokes}) between the absorption and the fluorescence peaks are also listed.

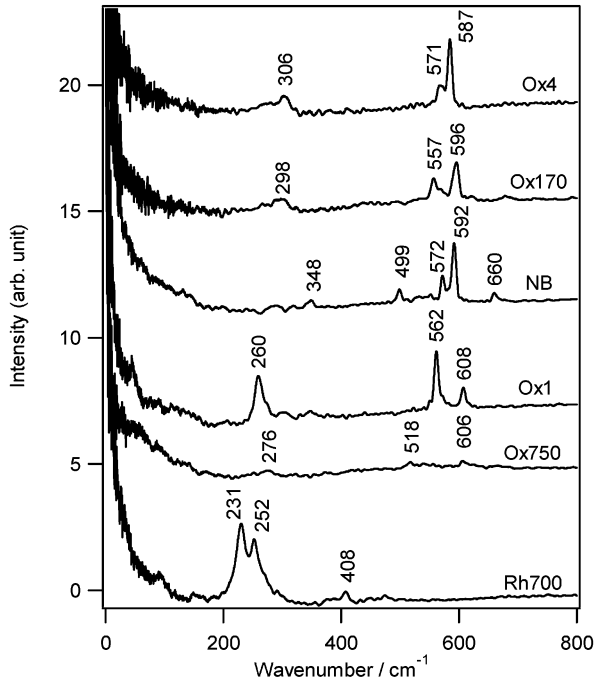

Figure 8. Real part of the Fourier-transformed spectra of the PP signals of xanthene dyes in methanol solution.

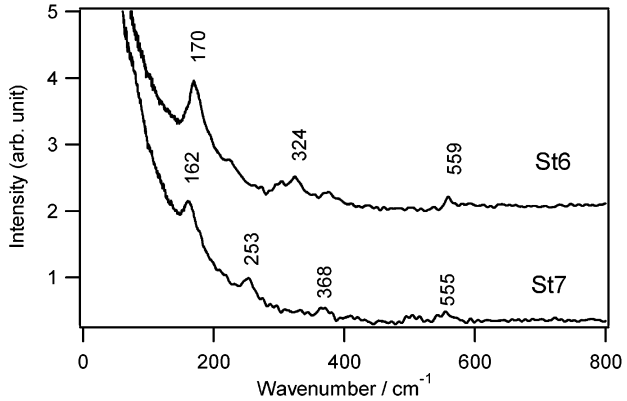

Figure 9. Real part of the Fourier-transformed spectra of the PP signals of styryl dyes in methanol solution.

fixed for Rh700. Note that Ox750 and Rh700 have the smallest initial peak shift and the fastest decay in the 3PEPS signal (Figure 5 and Table 1). It is possible that rotation of the free amino groups contributes to the picosecond decay of the 3PEPS signal. However, as it will be mentioned later, the small initial peak shift and the fast 3PEPS decay of Ox750 and Rh700 seems to be caused by fast relaxation of the vibrational excess energy on the excited state and also by the observation window effect. The saturated hexagonal alkyl ring may result in syn and anti conformational isomers as in the case of coumarin 153.[27] Because Rh700 has two saturated rings, it could have more than

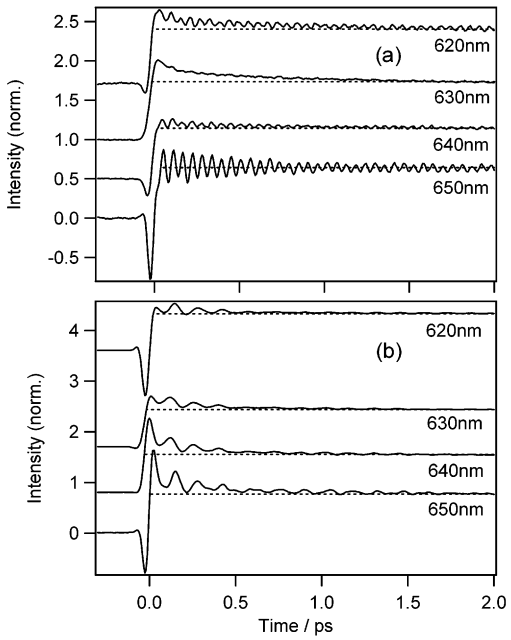

Figure 10. Wavelength-dependent detection of the PP signal of (a) Ox4 and (b) Rh700 in methanol.

three conformational isomers. However, the absorption bandwidth of Rh700 was the narrowest among the xanthene dyes, i.e., 950 cm^{-1} (fwhm), indicating the narrowest inhomogeneous broadening. The broadest absorption bandwidth was that of NB, which was ∼1800 cm^{-1} (fwhm). NB also had the largest Stokes shift among the xanthene dyes, i.e., ∼1820 cm^{-1} indicating the largest charge redistribution upon photoexcitation. Molecular structures of styryl dyes are more flexible than xanthene dyes, which can lead to cis−trans isomerization. It can be clearly seen from Figure 2 that bandwidths of the spectra and the Stokes shifts of styryl dyes are much larger than those of xanthene dyes, indicating stronger polar interaction with the solvent. Note that the fluorescence bandwidth of St6 is considerably narrower than that of the absorption, indicating a large conformational change upon photoexcitation.

The real parts of the Fourier-transformed spectra of the PP signals of the dyes, which correspond to the resonant Raman scattering spectra, are shown in Figures 8 and 9. For NB, 12 low-frequency Raman active modes below 700 cm^{-1} are known,[55] five of which were clearly observed in our Fourier-transformed spectrum. The strongest mode at 592 cm^{-1} was assigned to the ring breathing mode,[55] and similar modes are also observed around 560−600 cm^{-1} for other xanthene dyes except Rh700. For Ox750, Raman intensity was somehow extremely weak and the peaks are hardly detectable. For Rh700, there were two strong modes at lower frequencies of 231 and 525 cm^{-1}. Two low-frequency Raman active modes were reported for Ox1 in *N*,*N*-dimethylaniline, one strong and one weak at 567 and 608 cm^{-1}, respectively.[56] We observed similar

modes, although the frequency of the stronger mode was shifted down to 562 cm^{-1}. The frequency of this mode may be sensitive to solvent polarity or hydrophobicity. The mode of Ox4 (LD690) at 306 cm^{-1} was previously assigned to the vibration in the excited state, because it did not appear in the steady state resonant Raman spectrum.[57] However, it was observed in the resonance Raman spectrum obtained by another research group with a better S/N ratio.[58] Our result also supports that this mode originates from the ground state because the initial phase of this mode was equivalent to that of the ground state vibration at 587 cm^{-1} within experimental error. The low-frequency part of the resonance Raman spectrum of St7 (LDS750) was featured by broad bands around 300−500 cm^{-1} and a mode at 550 cm^{-1}.[58] We have observed modes at similar frequencies and an additional low-frequency mode at 162 cm^{-1}. A similar frequency of 173 cm^{-1} was observed as an oscillation in the transient PP signal of St7 in acetonitrile detected at 667 nm.[24] It was assigned to the ground state vibration because the oscillation persisted on a picosecond time scale, which was longer than the initial excited state lifetime. The frequencies of the modes observed in Figures 8 and 9 were utilized for the fitting of the 3PEPS signals.

4.2. 3PEPS Signals of Xanthene Dyes. 3PEPS signals of xanthene dyes are shown in Figure 5, which exhibit striking solute molecule dependence. The initial peak shift was larger in the order of Ox4 > Ox170 > NB > Ox1 > Rh700 > Ox750. The value of the asymptotic peak shift also decreased in similar order. The 3PEPS signal of Rh700 and Ox750 decayed immediately while those of Ox4 and Ox170 had longer decay components. The results of the fitting are shown in Table 1. The values of the third time constant, τ_3, were 8.4 ± 1.6 and 3.0 ± 0.3 ps for Ox4 and Ox170, respectively, while those of the rest of the molecules were 1.0−2.0 ps. The values of the second time constant, τ_2, were also long for Ox4 and Ox170 as compared to other dyes, which were 490 ± 90 and 400 ± 60 fs, respectively. When Figure 1 and Figure 5 are compared, a correlation can be found between the wavelengths of the maxima of electronic transition spectra and the 3PEPS signals. The peak wavelengths of the absorption and fluorescence spectra became longer in the order of Ox4 < Ox170 < NB < Ox1 < Rh700 < Ox750. Because the laser wavelength is fixed at 635 nm, the excited part of the absorption band will change from the blue side to the red side of the peak when the solute is changed in this order. When the blue side of the absorption spectrum is excited, the initial echo peak shift and the 3PEPS decay were smaller and faster, respectively. From another point of view, it can be said that solute molecules with larger overlap between fluorescence and laser spectrum had larger initial peak shift and slower 3PEPS decay. Note that there was no correlation between the 3PEPS decay and the bandwidth of the spectra or Stokes shift.

When the blue side of the absorption band is excited, it can be easily understood that the electronic transition will take place to higher vibrational levels of the excited state. Intramolecular vibrational redistribution (IVR) and VR in the excited state are considered to be extremely fast[3] and can affect the earlier part of the 3PEPS signal. This type of effect was already known for photon echo signals in low-temperature glasses. The excitation of higher lying vibrations can add a very fast component to the echo decay.[59] This can be minimized by exciting well to the red of the inhomogeneous absorption maximum.

Ippen and co-workers have carried out temperature dependence of the photon echo peak shift for dye molecules, cresyl violet, NB, and Ox170 in poly(methyl methacrylate) (PMMA).[51,60] An increase of the peak shift from 0 to 30 fs was observed for cresyl violet when the temperature was decreased from 290 to 15 K. However, for NB and Ox170, no peak shift was detected over the entire temperature range. The result was explained in terms of a multilevel vibrational structure. For NB and Ox170, the laser photons had in each case an excess energy of several hundred reciprocal centimeters relative to the absorption onset; for cresyl violet, however, the laser frequency was coincident with the absorption edge. Therefore, NB and Ox170 should have considerably higher densities of states than did cresyl violet. Because of higher densities of states, the dephasing appeared instantaneous.

Wavelength-dependent 3PEPS measurement of NB in acetonitrile carried out by Fleming and co-workers has also shown that the echo peak shift depends on excitation wavelength.[29,30] The entire echo peak shift decreased when the laser wavelength was tuned to the blue side of absorption. It was concluded that a detailed vibronic model for the chromophore is required for a detailed quantitative analysis of the solvation dynamics of chromophores immersed in nonreacting solvent. Their simulation showed that intramolecular high-frequency modes and their combination bands greatly contribute to the wavelength dependence of the 3PEPS decay, although the intuitive physical mechanism was not very explicit. It was concluded that experimental conditions that favor the extraction of solvation dynamics from photon echo peak shift measurements include excitation on the red edge of the absorption band and the use of short, transform-limited pulses.

However, these mechanisms may not fully explain the observed phenomena. Previous 3PEPS experiments have shown that the picosecond decay can be assigned to the diffusive solvation process because it depends strongly on solvent and it becomes infinitely long in polymer glasses. The time constants of the picosecond decay components were 8.4 ± 1.6 and 3.0 ± 0.3 ps for OX4 and Ox170, respectively, and they were clearly slower than those of other xanthene dyes. To explain such a large difference in picosecond decay, two new mechanisms have to be considered, which are nonlinear coupling and observation window effect. Experimentally observed correlation functions such as $S(t)$ and $W(t)$ are equivalent to solvent fluctuation correlation function of the transition frequency, $M(t)$, only when linear coupling and high-temperature limit approximations are valid. Moreover, experimentally observable phenomena can only be limited in the observation window determined by the laser bandwidth. Phenomena occurring at wavelengths outside of the laser spectrum cannot be observed. Scheme 2 depicts such a situation. The curves represent the free energy surfaces in the excited and ground states of the solute molecule along the solvation coordinate. Initially, only the ground state is populated and the excitation pulse creates a hole and an antihole in the ground and in the excited states, respectively. After the excitation, relaxation toward thermal equilibrium will take place on both energy surfaces. When the blue side of the absorption band is excited (Scheme 2a), the population will be generated away from the energy minimum on the excited state surface. In this case, both population shift and broadening have to take place for thermal relaxation in the excited state. On the other hand, when the red side of the absorption is excited, the population will be generated closer to the minimum and mainly the broadening will take place. In the case of Scheme 2a, the population generated on the excited state can shift away from the experimental observation window with time, while in the case of Scheme 2b, the population always stays close to the observation window. Moreover, in the case of Scheme 2a, the

SCHEME 2: Free Energy Diagrams along the Solvation Coordinate[a]

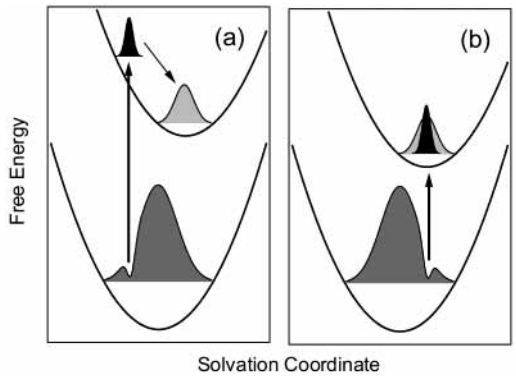

[a] When the blue side of the absorption spectrum is excited (a), initial population is generated away from the minimum of the free energy surface of the excited state. Thermal relaxation involves both the shift and the broadening of the population. When the red side of the absorption spectrum is excited (b), initial population is generated close to the minimum of the free energy surface of the excited state. Thermal relaxation in the excited state involves mainly the broadening of the population.

experiment will monitor mainly the $S(t)$ contribution in the excited state, while in the case of Scheme 2b, it will monitor mainly the $W(t)$ contribution. If the linear coupling approximation does not hold, these two cases may result in different experimentally observed correlation functions. In these discussions, ground state dynamics was assumed to be similar for both cases.

The difference between spectral shift and broadening functions had been observed by Nishiyama and Okada for time-resolved hole burning and FDSS.[11,61] Their data showed that the spectral shift occurred faster than the broadening. Theoretically, Yoshimori showed that spectral broadening and shift can exhibit different dynamics in the presence of nonlinear coupling, when the dynamics of the solvent number density and the orientational relaxation are considered.[62,63] It should also be mentioned that unharmonicity of the free energy surface can also contribute to such an effect. Unharmonicity is known to be caused along the solvation coordinate by dielectric saturation in the case of charge separation reaction.[64,65]

All of the measured 3PEPS signals had a decay component with extremely long time constant, i.e., $\gg$100 ps. Such a slow solvation process has never been observed for methanol with other experimental methods, although similar slow dynamics have been observed by 3PEPS measurements for methanol and other simple fluid solvents. Lee et al. have measured the 3PEPS signal of a dye, DTTCI, in methanol up to 500 ps and concluded that the asymptotic peak shift decayed with a time constant of 1.5 ns.[66] The longest time constant measured for methanol was 15 ps by time-resolved FDSS using coumarin 153 as a probe molecule.[3] Because measurable time range is limited by the excited state lifetime for this method, such a slow process might have been missed. However, even with dielectric dispersion measurement, the longest time constant of methanol was ~160 ps.[3,67] Lee et al. concluded that because DTTCI is a large and flexible molecule, it is possible that the nanosecond component may be originated from the solute's equilibrium conformational inhomogeneity, i.e., the origin is intramolecular. In this scenario, the nanosecond component accounts for the time scale of the solute's equilibrium geometry fluctuation, and the time-resolved fluorescence Stokes shift measurement should not be sensitive to this process. Similar intramolecular inhomogeneity may be present for xanthene dyes, although xanthene dyes are much more rigid molecules than DTTCI. If we could expand the experimental time range, we might be able to observe the difference in the relaxation time for this slow component due to structural difference. A similar slow component was also observed by 3PEPS measurements utilizing IR144 and DTTCI in other simple fluid solvents such as acetonitrile.[16,17,34,35] In our analysis, this slow component was not included in the experimentally obtained correlation function, $M(t)$, shown in Figure 11a, because its origin may be intramolecular and compared with other correlation functions obtained by different methods.

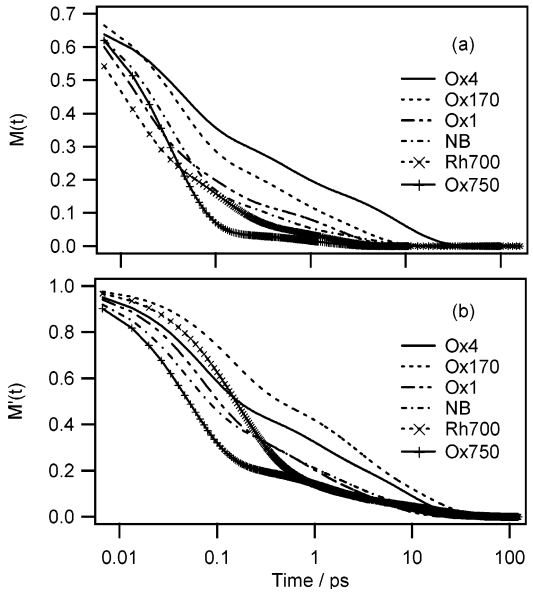

Figure 11. (a) Experimental solvent correlation function, $M(t)$, obtained by the 3PEPS measurements of xanthene dyes. (b) The normalized dynamics of the PP signals of xanthene dyes faster than the excited state lifetime depicted as $M'(t)$.

4.3. Comparison of Xanthene 3PEPS Data with Other Experimental Results. The longest picosecond decay component obtained for methanol was 8.4 ± 1.6 ps with Ox4 in our experimental results. This value is quite similar to the ones obtained by other 3PEPS measurements using different probe molecules such as IR144 and DTTCI. The longest picosecond components obtained with IR144 and DTTCI are 9.5−11 and 5−9.5 ps, respectively.[16,17,34,35,66] However, the longest picosecond component obtained by FDSS measurement using coumarin 153 was slightly longer, i.e., 15.3 ps.[3] To check whether this discrepancy is of any significance, we will take a look at the results of other solvents. For acetonitrile, picosecond time constants of 2−3 and 0.6−1 ps were obtained from 3PEPS and FDSS measurements, respectively.[3,34,35,66] For benzonitrile, ethanol, and 1-butanol, values of 15, 20−27, 33 ps were obtained from 3PEPS measurement, while values of 25, 30, and 133 ps were obtained from FDSS measurements, respectively.[3,17,34,35,68] There seems to be a tendency of the time constants obtained by 3PEPS measurements to be slightly shorter than those obtained by FDSS measurements with an exception of acetonitrile.

It should be pointed out that the accuracy of these values depends on the experimentally measured time range. If the time range is too short, the measurement can miss some slow decay. It also may be that because the observation window of 3PEPS measurement is limited by the laser bandwidth, while FDSS measurement monitors the entire fluorescence spectrum, 3PEPS measurement might have missed some portion of the relaxation process. Another possibility that should be considered is the

TABLE 2: Time Constants (τ_i) and Amplitudes (A_i) of the Decay Components Obtained from the Nonlinear Least-Squares Fitting of the PP Signals

	Ox4	Ox170	NB	Ox1	Rh700	Ox750	St7	St6
τ_1 (fs) (A_1)	67 ± 0 (0.19)	130 ± 0 (0.14)	44 ± 2 (0.30)	66 ± 21 (0.35)	150 ± 10 (0.25)	50 ± 0 (0.27)	61 ± 1 (0.59)	40 ± 5 (0.17)
τ_2 (fs) (A_2)	860 ± 30 (0.08)		310 ± 10 (0.10)	630 ± 20 (0.13)	650 ± 80 (0.06)		360 ± 10 (0.17)	130 ± 0 (0.44)
τ_3 (ps) (A_3)		2.1 ± 0.1 (0.09)	1.9 ± 0.1 (0.10)	4.4 ± 0 (0.12)		1.2 ± 0 (0.05)	1.7 ± 0.1 (0.10)	1.1 ± 0 (0.12)
τ_4 (ps) (A_4)	8.6 ± 0.2 (0.11)	13 ± 1 (0.08)	12 ± 0 (0.06)		8.9 ± 0.8 (0.04)	16 ± 1 (0.03)	7.7 ± 0.4 (0.08)	7.9 ± 0.2 (0.10)
τ_5 (ps) (A_5)	≫100 (0.62)	≫100 (0.69)	≫100 (0.44)	≫100 (0.40)	≫100 (0.65)	≫100 (0.65)	120 ± 17 (0.06)	40 ± 0 (0.17)

difference that FDSS measurement requires probe molecules with large Stokes shift (polar systems), while 3PEPS measurement requires ones with small Stokes shifts (nonpolar or weakly polar systems). The value of Stokes shift depends on the strength of coupling between solvent fluctuation and electronic transition. In the presence of nonlinear coupling, solute molecules with different coupling strengths can exhibit different time constants.

Also, a 3PEPS trace at ultrashort time scale does not reflect the time scales of actual dynamics, i.e., eq 4 is not accurate at ultrashort time scales (≤100 fs). Thus, $M(t)$ obtained by simply fitting the 3PEPS trace cannot be directly compared to $S(t)$ obtained by FDSS measurements. Detailed numerical modeling is required to extract the short time behavior of $M(t)$. Another discrepancy between 3PEPS and FDSS measurement is caused by the difference in the pulse duration. 3PEPS measurement can utilize optical pulses as short as 20 fs or shorter, while FDSS measurement is usually carried out with pulses with duration of ~100 fs or longer. When the shorter pulse is used, greater numbers of vibrational modes can be coherently excited. These coherent oscillations will interfere constructively at time origin, while slight deviation from the time origin will cause them to interfere destructively, resulting in an ultrafast decay. Therefore, the ultrafast part of $M(t)$ obtained from 3PEPS measurement is usually more enhanced than $S(t)$ obtained from dynamic Stokes shift measurement.

To consider the effect of observation window, we have carried out a comparison between 3PEPS and PP measurements. Fitting was carried out using multiexponential decay and multiple oscillations for PP signals of xanthene dyes, of which the obtained time constants are listed in Table 2. Frequencies obtained from the Fourier transform spectra of the PP signals were used again in the fitting procedure. Dynamics faster than the excited state lifetime obtained by PP measurements are normalized and depicted as $M'(t)$ in Figure 11b. There seems to be a correlation between $M(t)$ obtained from 3PEPS measurement and $M'(t)$ obtained from PP measurement, i.e., the decay was the slowest for Ox4 and Ox170, while it was the fastest for Ox750 and Rh700. This result strongly suggests that observable phenomena with 3PEPS measurement are limited in the observation window defined by the laser bandwidth.

To elucidate the origin of the fast decay components in the PP signal, wavelength-dependent detection of the PP signal was carried out, and the results are shown in Figure 10 for Ox4 and Rh700. When the detection wavelength was tuned to the edge of the laser spectrum, a sharp dip appeared in the signal right before the time origin. This dip seems to be the effect of the coherent interference of the signal, which occurs when pump and probe pulses are overlapped. The oscillations also got stronger when the detection wavelength was tuned to the edge of the laser spectrum. These features are commonly observed for wavelength-resolved PP signals.[69] It is interesting to see that the fast decay components appeared at shorter wavelengths for Ox4, while they appeared at longer wavelengths for Rh700. Comparing this result with the electronic transition spectra shown in Figure 1, it can be noticed that the fast decay component appeared when the detection wavelength was overlapped with the blue side of the fluorescence spectrum. For Ox4, the blue side of the fluorescence spectrum was positioned at the blue side of the laser spectrum, while for Rh700, it was positioned at the red side of the laser spectrum. It is known from the up-conversion measurement of fluorescence spectrum that dynamic Stokes shift causes fast decay on the blue side of the fluorescence spectrum, while it causes a rise of the fluorescence intensity on the red side.[1,3,7,68] It can be assumed that the fast decay components observed in our PP measurements originated from the FDSS. This result supports our conclusion that fast decay of the 3PEPS signal is caused by the dynamics in the excited state. It should be considered why 3PEPS measurement is so sensitive to the excited state dynamics while it is not to the ground state ones. Because the ultrashort laser bandwidth is so wide (~30 nm at fwhm) and so many numbers of vibrational modes exist for a dye molecule, the hole burned in the ground state absorption band may be so wide that broadening is not effectively detectable. The only detectable time-dependent change may be the dynamic Stokes shift on the excited state, although this assumption needs further investigation.

Recently, Yu et al. have carried out static solvatochromic studies and PP measurements of three structurally related cynanine dyes, HDITCP, IR125, and IR144.[70] From the static measurements, it was concluded that HDITCP and IR125 show classical nonpolar solvatochromism, while IR144 shows polar solvatochromism, which can be attributed to a dipole decrease upon photoexcitation. PP signals of HDITCP and IR144 were compared, and it was observed that amplitudes and decay time constants of the solvation dynamics were larger and longer for IR144. Because nonpolar solvation originates from weak short-range viscoelastic interaction while polar solvation originates from strong long-range dielectric interaction, polar solvation is expected to have a larger amplitude and slower relaxation. The PP signal of IR144 also exhibited a strong coherent spike near the time origin, which was attributed to the inertial polar solvation response. Because Stokes shifts of styryl dyes are much larger than those of xanthene dyes (Figures 1 and 2 and Table 1), it can be said that polar solvation is dominant for styryl dyes. A stronger coherent spike appearing in the PP signals of styryl dyes as compared to xanthene dyes (Figure 7) supports this conclusion. Among the xanthene dyes, NB has the largest Stokes shift (914 cm^{-1}) and Ox750 has the smallest one (378 cm^{-1}). Therefore, larger amplitudes and slower decays observed in the 3PEPS signal of NB can be partially due to the stronger contribution from polar solavtion mechanism (the same trend can be also observed in the $M'(t)$ obtained from PP measurement). However, it should be noted that Ox4, which has a smaller value of Stokes shift than NB (594 cm^{-1}), exhibits larger amplitude and slower decay in the 3PEPS signal (Figure 5). Therefore, the ratio between polar and nonpolar solvation is not the only factor that determines the decay of the 3PEPS signal.

Although the solute dependence of 3PEPS and PP signals had similar tendencies, the solvation time constants obtained from PP measurement were noticeably longer than the ones

obtained from 3PEPS measurement. A similar trend can also be seen in the measurements of Yu et al., i.e., decay times of IR144 obtained from PP measurements were always longer than those obtained from 3PEPS measurements.[70] For low-temperature optical-dephasing measurements of glassy solids, it is known that photon echo is only sensitive to a fast optical-dephasing process caused by phonon-assisted tunneling, while hole burning is sensitive to a slower spectral diffusion process.[59] According to Zhang and Berg, PP measurement can also be termed as single wavelength transient hole burning.[12] It can be that PP measurement is more sensitive to slower dynamics than 3PEPS measurement by analogy to the low-temperature optical-dephasing measurements. Zhang and Berg have recently claimed the advantage of PP measurement over 3PEPS measurement.[12] They have shown that PP signal can be approximated by a rather lengthy algebraic formula containing a slower part of $M(t)$ and simple fitting of the PP decay can recover time scales similar to $M(t)$ in the weak coupling case (nonpolar solvation). However, in the case of strong coupling (polar solvation), time scales obtained from the simple fitting resulted in significantly shorter time scales than $M(t)$ because the population moves out of resonance with the laser frequency (observation window) due to larger dynamic Stokes shift. Their conclusion is consistent with ours and indicates that a larger coherent spike observed in the PP signal for styryl dyes as compared to xanthene dyes (and also for IR144 as compared to HDITCP[70]) is due to the limited observation window.

4.4. 3PEPS Signals of Styryl Dyes. 3PEPS measurement of St6 was only possible up to 10 ps because of its short excited state lifetime (Figure 6a). The 3PEPS signal decayed very rapidly similar to those of Ox750 and Rh700. This rapid decay can also be explained by the observation window effect. As can be seen from Figure 2, the Stokes shift between the absorption and the fluorescence peak is very large for St6 and the laser spectrum is located at the blue edge of the fluorescence spectrum. Thus, the initial population generated on the excited state on photoexcitation will rapidly move out of the observation window, causing the 3PEPS signal to decay rapidly.

The 3PEPS signal of St7 was more confusing because after the rapid decay, it started to increase again in the picosecond range. The time constant of this rise is not so accurate, probably more than 16 ps, because 3PEPS measurement was only possible up to 50 ps. Such a rise has never been observed in simple solvent−solute systems but in a bacterial photosynthetic reaction center.[50] 3PEPS measurement was carried out on the accessory bacteriochlorophyls (Bchl) in the reaction center of *Rhodobacter sphaeroides*. In this complex system, photoexcitation of the accessory Bchls leads to energy transfer to the primary electron donor, which is a pair of closely interacting Bchls, with a time constant of 80−130 fs. Subsequently, charge separation takes place from the primary electron donor to the bacteriopheophytin in ∼3 ps. Increase of the peak shift with a time constant of 2.8 ps was observed in the 3PEPS signal, and it was explained by the decay of the excited state of the primary electron donor as the charge-separated state is formed and the subsequent recovery of the echo signal from the ground state of the accessory Bchls. The increase may also be due to the electrochromic shift of the absorption band of the accessory Bchl due to formation of the charge-separated state. Theoretically, it was shown that rapid decay of the excited state and rapid recovery of the ground state in two or three level systems can lead to an increase of the peak shift in 3PEPS signal.[71] Because St7 is known to undergo ultrafast photoisomerization, formation of the isomer can lead to the increase of the echo peak shift.

The ultrafast inertial contribution to the solvation dynamics was first observed by St7 (LDS750) dissolved in acetonitrile.[22] However, it was pointed out that such a floppy molecule may not be appropriate as a solvatochromic probe. The transient absorption measurement was carried out for St7, and it was concluded that an intramolecular process dominates the observed Stokes shift.[24] The first excited electronic state isomerizes in an ultrafast process followed by a slower process, the dynamics of which is controlled by the solvent. Bardeen et al. have also measured temperature dependence of the photon echo signal of St7 in PMMA.[72] Its optical-dephasing rate was close to pulse width-limited and was almost completely insensitive to temperature from 240 to 28 K. Furthermore, St7's dephasing rate depended strongly on the population period, becoming pulse width-limited by 100 fs. In other words, St7 was subject to a very large perturbation very quickly upon excitation, which led to rapid loss of phase memory. It was considered that this perturbation may be the result of some fast intramolecular relaxation or isomerization. The vibrational spectrum of St7 was considerably complex, indicating that the optical transition is strongly coupled to many vibrational modes. It was also considered that large charge redistribution upon photoexcitation in St7 could result in a strong coupling to the environmental fluctuations that the temperature dependence is difficult to observe even with time resolution of 10 fs.

The increase of the echo peak shift observed in the 3PEPS signal had a time constant of ∼16 ps, which was much slower than that of the isomerization of St7 previously observed by transient absorption and photon echo measurements. The isomerization was assumed to occur with an average time constant of ∼200 fs in acetonitrile and causes the red shift of the fluorescence spectrum. [24] The fluorescence of the final excited state, which is the isomeric form of the molecule, peaks at ∼720 nm. Thus, the initial isomerization process can be partially involved in the ultrafast decay of the 3PEPS signal. If the isomer formed in the excited state transforms into a ground state isomer, which absorbs around 635 nm, with a time constant of ∼16 ps, the formation of the ground state isomer may contribute as a rise in the 3PEPS signal. The formation of the isomer in the ground state can be regarded as an increase of structural inhomogeneity of the solute molecule and thus results as an increase of the peak shift. It should be mentioned that if 3PEPS measurement was possible up to 50 ps, a similar increase of the echo peak shift might have also appeared for St6.

5. Conclusions

The dependence of the 3PEPS signal on probe solute molecules was studied using several xanthene dyes and styryl dye molecules in methanol and compared with PP measurements. For xanthene dyes, the decay was faster when the blue side of the absorption spectrum was excited. This effect was considered to be the result of a limited observation window and VR of the excess energy on the excited state through higher density of states. The effects of nonlinear coupling between electronic transition and solvent fluctuation or the unharmonicity of the free energy surface are also considered, although further investigation is necessary. For styryl dyes, a gradual increase of the peak shift was observed in the picosecond region, which may be the result of photoinduced isomerization. It seemed that the 3PEPS signal was more sensitive to the excited state dynamics rather than to the ground state ones because the bandwidth of the femtosecond laser was so wide (∼30 nm) that the hole created in the ground state was too large for effective observation of the hole broadening.

Finally, we would like to compare advantages and disadvantages of 3PEPS, PP, and FDSS measurements. For systems with small Stokes shifts (nonpolar or weakly polar case), 3PEPS and PP measurements are reliable methods to determine solvation dynamics, if the laser frequency is set close to the 0−0 transition of the chromophore. The PP measurement is expected to have the highest accuracy, because a large number of points can be measured in shorter times; however, $M(t)$ cannot be directly obtained from the signal decay. For the systems with large Stokes shifts (strongly polar case), 3PEPS and PP measurements are not reliable because of the limited observation window. For strongly polar systems, DFSS measurement seems to be the only reliable method. One advantage of 3PEPS measurement that others do not have is the sensitivity to extremely slow dynamics (or static inhomogeneity), which will be masked by the excited state decay for PP and DFSS measurements. A comprehensive application of these methods can open a door to better understanding of polar and nonpolar contribution (or nonlinear and unharmonic contribution) to the solvation dynamics.

Acknowledgment. This research was supported by a Grant-in-Aid for Specially Promoted Research (No. 10102007) from the Ministry of Education, Culture, Sports, Science and Technology of Japan, and the development of the Cr:F laser was partially supported by Sumitomo Foundation. Y.N. thanks Dr. D. Larsen, R. Jimenez, and K. Ohta for stimulating discussions and Ms. Y. Nakagawa and Mr. Y. Mori for assistance with the experiment.

References and Notes

(1) Barbara, P. F.; Jarzeba, W. In *Advances in Photochemistry*; Voman, D. H., Hammond, G. S., Gollnick, K., Eds.; A Wiley-Interscience Publication: New York, 1990; Vol. 15, p 1.
(2) Heitele, H. *Angew. Chem., Int. Ed. Engl.* **1993**, *32*, 359.
(3) Horng, M. L.; Gardecki, J. A.; Papazyan, A.; Maroncelli, M. *J. Phys. Chem.* **1995**, *99*, 17311.
(4) Kahlow, M. A.; Jarzeba, W.; DuBruil, T. P.; Barbara, P. F. *Rev. Sci. Instrum.* **1988**, *59*, 1098.
(5) Jimenez, R.; Fleming, G. R.; Kumar, P. V.; Maroncelli, M. *Nature* **1994**, *369*, 471.
(6) Maroncelli, M. *J. Mol. Liq.* **1993**, *57*, 1.
(7) Maroncelli, M.; Flemming, G. R. *J. Chem. Phys.* **1987**, *86*, 6221.
(8) Rosenthal, S. J.; Jimenez, J.; Fleming, G. R. *J. Mol. Liq.* **1994**, *60*, 25.
(9) Yoshihara, K.; Tominaga, K.; Nagasawa, Y. *Bull. Chem. Soc. Jpn.* **1995**, *68*, 697.
(10) Fourkas, J. T.; Berg, M. *J. Chem. Phys.* **1993**, *98*, 7773.
(11) Nishiyama, K.; Okada, T. *J. Phys. Chem. A* **1997**, *101*, 5729.
(12) Zhang, Y.; Berg, M. A. *J. Chem. Phys.* **2001**, *115*, 4223.
(13) Agarwal, R.; Prall, B. S.; Rizvi, A. H.; Yang, M.; Fleming, G. R. *J. Chem. Phys.* **2002**, *116*, 6243.
(14) de Boeij, W. P.; Pshenichnikov, M. S.; Wiersma, D. A. *Chem. Phys.* **1998**, *233*, 287.
(15) Joo, T.; Jia, Y.; Fleming, G. R. *J. Chem. Phys.* **1995**, *102*, 4063.
(16) Joo, T.; Jia, J.; Yu, J.-Y.; Lang, M. J.; Fleming, G. R. *J. Chem. Phys.* **1996**, *104*, 6089.
(17) de Boeij, W. P.; Pshenichnikov, M. S.; Wiersma, D. A. *J. Phys. Chem.* **1996**, *100*, 11806.
(18) de Boeij, W. P.; Pshenichnikov, M. S.; Wiersma, D. A. *J. Chem. Phys.* **1996**, *105*, 2953.
(19) Kinoshita, S.; Nishi, N. *J. Chem. Phys.* **1988**, *89*, 6612.
(20) Cho, M.; Yu, J.-Y.; Joo, T.; Nagasawa, Y.; Passino, S. A.; Fleming, G. R. *J. Phys. Chem.* **1996**, *100*, 11944.
(21) de Boeij, W. P.; Pshenichnikov, M. S.; Wiersma, D. A. *Chem. Phys. Lett.* **1996**, *253*, 53.
(22) Rosenthal, S. J.; Xie, X.; Du, M.; Fleming, G. R. *J. Chem. Phys.* **1991**, *95*, 4715.
(23) Blanchard, G. J. *J. Chem. Phys.* **1991**, *65*, 6317.
(24) Kovalenko, S. A.; Ernsting, N. P.; Ruthmann, J. *J. Chem. Phys.* **1997**, *106*, 3504.
(25) Jiang, Y.; MacCarthy, P. K.; Blanchard, G. J. *Chem. Phys.* **1994**, *183*, 249.
(26) Kovalenko, S. A.; Ruthmann, J.; Ernsting, N. P. *Chem. Phys. Lett.* **1997**, *271*, 40.
(27) Pryor, B. A.; Palmer, P. M.; Chen, Y.; Topp, M. R. *Chem. Phys. Lett.* **1999**, *299*, 536.
(28) Chapman, C. F.; Fee, R. S.; Maroncelli, M. *J. Phys. Chem.* **1995**, *99*, 4811.
(29) Larsen, D. S.; Ohta, K.; Xu, Q.-H.; Cyrier, M.; Fleming, G. R. *J. Chem. Phys.* **2001**, *114*, 8008.
(30) Ohta, K.; Larsen, D. S.; Yang, M.; Fleming, G. R. *J. Chem. Phys.* **2001**, *114*, 8020.
(31) Lang, M. J.; Jordanides, X. J.; Song, X.; Fleming, G. R. *J. Chem. Phys.* **1999**, *110*, 5884.
(32) Larsen, D. S.; Ohta, K.; Fleming, G. R. *J. Chem. Phys.* **1999**, *111*, 8970.
(33) Fleming, G. R.; Cho, M. *Annu. Rev. Phys. Chem.* **1996**, *47*, 109.
(34) Passino, S. A.; Nagasawa, Y.; Joo, T.; Fleming, G. R. *J. Phys. Chem.* **1997**, *101*, 725.
(35) Passino, S. A.; Nagasawa, Y.; Fleming, G. R. *J. Chem. Phys.* **1997**, *107*, 6094.
(36) Fleming, G. R.; Passino, S. A.; Nagasawa, Y. *Philos. Trans. R. Soc. London A* **1998**, *536*, 389.
(37) de Boeij, W. P.; Pshenichnikov, M. S.; Wiersma, D. A. *Chem. Phys. Lett.* **1995**, *238*, 1.
(38) Kennis, J. T. M.; Larsen, D. S.; Ohta, K.; Facciotti, M. T.; Glaeser, R. M.; Fleming, G. R. *J. Phys. Chem. B* **2002**, *106*, 6067.
(39) Jordanides, X. J.; Lang, M. J.; Song, X.; Fleming, G. R. *J. Phys. Chem. B* **1999**, *103*, 7995.
(40) Homoelle, B. J.; Edington, M. D.; Diffey, W. M.; Beck, W. F. *J. Phys. Chem. B* **1998**, *102*, 3044.
(41) Jimenez, R.; Case, D. A.; Romesberg, F. E. *J. Phys. Chem. B* **2002**, *106*, 1090.
(42) Joo, T.; Jia, Y.; Yu, J.-Y.; Jonas, D. M.; Fleming, G. R. *J. Phys. Chem.* **1996**, *100*, 2399.
(43) Jimenez, R.; van Mourik, F.; Yu, J. Y.; Fleming, G. R. *J. Phys. Chem. B* **1997**, *101*, 7350.
(44) Yu, J.-Y.; Nagasawa, Y.; van Grondelle, R.; Fleming, G. R. *Chem. Phys. Lett.* **1997**, *280*, 404.
(45) Salverda, J. M.; van Mourik, F.; van der Zwan, G.; van Grondelle, R. *J. Phys. Chem. B* **2000**, *104*, 11395.
(46) Agarwal, R.; Krueger, B. P.; Scholes, G. D.; Yang, M.; Yom, J.; Mets, L.; Fleming, G. R. *J. Phys. Chem. B* **2000**, *104*, 2908.
(47) Agarwal, R.; Yang, M.; Xu, Q.-H.; Fleming, G. R. *J. Chem. Phys. B* **2001**, *105*, 1887.
(48) Yang, M.; Fleming, G. R. *J. Chem. Phys.* **1999**, *111*, 27.
(49) Yang, M.; Fleming, G. R. *J. Chem. Phys.* **2000**, *113*, 2823.
(50) Groot, M.-L.; Yu, J.-Y.; Agarwal, R.; Norris, J. R.; Fleming, G. R. *J. Phys. Chem. B* **1998**, *102*, 5923.
(51) Weiner, A. M.; De Silvestri, S.; Ippen, E. P. *J. Opt. Soc. Am. B* **1985**, *2*, 654.
(52) Nagasawa, Y.; Ando, Y.; Watanabe, A.; Okada, T. *Appl. Phys. B* **2000**, *70* (Suppl.), S33.
(53) Nagasawa, Y.; Passino, S. A.; Joo, T.; Fleming, G. R. *J. Chem. Phys.* **1997**, *106*, 4840.
(54) Nagasawa, Y.; Ando, Y.; Kataoka, D.; Matsuda, H.; Miyasaka, H.; Okada, T. *J. Phys. Chem. A* **2002**, *106*, 2024.
(55) Lawless, M. K.; Mathies, R. A. *J. Chem. Phys.* **1992**, *96*, 8037.
(56) Engleitner, S.; Seel, M.; Zinth, W. *J. Phys. Chem. A* **1999**, *103*, 3013.
(57) Hong, Q.; Pexton, I. A. D.; Porter, G.; Klug, D. R. *J. Phys. Chem.* **1993**, *97*, 12561.
(58) Bardeen, C. J.; Rosenthal, S. J.; Shank, C. V. *J. Phys. Chem. A* **1999**, *103*, 10506.
(59) Narasimhan, L. R.; Littau, K. A.; Pack, D. W.; Bai, Y. S.; Elschner, A.; Fayer, M. D. *Chem. Rev.* **1990**, *90*, 439.
(60) De Silvestri, S.; Weiner, A. M.; Fujimoto, J. G.; Ippen, E. P. *Chem. Phys. Lett.* **1984**, *112*, 195.
(61) Nishiyama, K.; Asano, Y.; Hashimoto, N.; Okada, T. *J. Mol. Liq.* **1995**, *65/66*, 41.
(62) Yoshimori, A. *J. Chem. Phys.* **1996**, *105*, 5971.
(63) Yoshimori, A.; Day, T. J. F.; Patey, G. N. *J. Chem. Phys.* **1998**, *109*, 3222.
(64) Kakitani, T.; Mataga, N. *Chem. Phys. Lett.* **1986**, *124*, 437.
(65) Tachiya, M. *Chem. Phys. Lett.* **1989**, *159*, 505.
(66) Lee, S.-H.; Lee, J.-H.; Joo, T. *J. Chem. Phys.* **1999**, *110*, 10969.
(67) Barthel, J.; Bachhuber, K.; Buchner, R.; Hetzenauer, H. *Chem. Phys. Lett.* **1990**, *165*, 369.
(68) Jarzeba, W.; Walker, C. G.; Johnson, A. E.; Barbara, P. F. *Chem. Phys.* **1991**, *152*, 57.
(69) Yang, T.-S.; Chang, M.-S.; Chang, R.; Hayashi, M.; Lin, S. H.; Vohringer, P.; Dietz, W.; Scherer, N. F. *J. Chem. Phys.* **1999**, *110*, 12070.
(70) Yu, A.; Tolbert, C. A.; Farrow, D. A.; Jonas, D. M. *J. Phys. Chem. A* **2002**, *106*, 9407.
(71) Yang, M.; Ohta, K.; Fleming, G. R. *J. Chem. Phys.* **1999**, *110*, 10243.
(72) Bardeen, C. J.; Cerullo, G.; Shank, C. V. *Chem. Phys. Lett.* **1997**, *280*, 127.